Forest-Cover–Type Separation Using RADARSAT-1 Synthetic Aperture Radar Imagery

Mark D. Nelson[1], **Kathleen T. Ward**[2], **and Marvin E. Bauer**[3]

Abstract.—RADARSAT-1 synthetic aperture radar data, speckle reduction, and texture measures provided for separation among forest types within the Twin Cities metropolitan area, MN, USA. The highest transformed divergence values for 16-bit data resulted from speckle filtering while the highest values for 8-bit data resulted from the orthorectified image, before and after performing a histogram stretch. First-order texture derivatives of 8-bit data provided only modest separability, while second-order texture derivatives of 8-bit data provided little, if any, separability. RADARSAT-1 imagery may provide for image separation among forest types provided that preexisting forest/nonforest land cover classifications are incorporated.

Introduction

The classification of forest land cover types from remotely sensed imagery is important for enhancing forest assessments. For example, a forest-cover–type map of the United States derived from Advanced Very High Resolution Radiometer (AVHRR) satellite imagery was used to supplement the Forest and Rangeland Renewable Resources Planning Act of 1974 (which was amended in 1992) Forest Resources Assessment (Powell *et al.* 1993, Zhu and Evans 1994). Päivinen *et al.* (2001) describe a more recent effort to combine AVHRR data with European forest statistics. The utility of these forest-cover–type maps depends on their classification accuracy and their correspondence with inventory-based forest assessments. Thus, developing approaches for improving forest-cover–type classifications provides significant value to forest assessment.

Optical sensors provide the source imagery for most forest-cover–type mapping efforts, but imagery collected by the sensors can be adversely affected by sun angle and atmospheric properties (e.g., clouds, haze, aerosols). Active radar signals are unaffected by these factors, but are sensitive to the moisture content and structural properties of vegetation. Satellite-borne synthetic aperture radar (SAR) data has potential for separating classes of land cover, especially when integrated with optical sensor data (Huang *et al.* 2007).

Imaging radar systems typically are categorized by microwave bands, with the following frequencies and wavelengths representing centers for each of four common bands: P-band (440 MHz, 65 cm λ), L-band (1.25 GHz, 24 cm λ), C-band (5.3 GHz, 5.6 cm λ), and X-band (10 GHz, 3.0 cm λ) (Kasichke *et al.* 1997). Each microwave band is differentially backscattered by objects approximately equal in size to the band's wavelength (Ranson and Williams 1992). Microwave scattering and attenuation in C-band SAR results from interactions with tree canopy leaves, needles, and small secondary branches, but C-band backscatter from tree trunks is small due to minimal canopy penetration (Kasichke *et al.* 1997). C-band SAR data does poorly at discriminating conifer from deciduous forest but shows good capabilities for differentiating some specific northern/temperate forest types (Leckie and Ranson 1998).

SAR data consists of backscatter or intensity values (strength of signal return) and texture (variability of backscatter within adjacent groups of pixels). SAR image texture consists of two components: speckle fluctuations and backscatter fluctuations. Speckle results in a grainy, salt-and-pepper appearance in SAR

[1] Research Forester, U.S. Department of Agriculture (USDA) Forest Service, Northern Research Station, St. Paul, MN.
[2] Forester, USDA Forest Service, Northern Research Station, St. Paul, MN.
[3] Professor, College of Food, Agricultural and Natural Resource Sciences, University of Minnesota, St. Paul, MN.

data. Speckle reduction is recommended prior to performing radar image processing (Collins *et al.* 2000). When analyzing SAR imagery, texture elements can be as important as backscatter data. SAR texture information is derived from first-order texture measures, such as moving window analysis and second-order statistics calculated from the Gray Level Co-occurrence Matrix (GLCM) (Haralick *et al.* 1973).

In summary, C-band SAR data achieves only moderate success at discriminating forest types and is even less useful for discriminating forest from nonforest. C-band SAR, however, may aid in discriminating among tree species when analyses are constrained to previously identified forested pixels and when speckle filtering and texture information are incorporated. In this study we assess the utility of RADARSAT-1 C-band SAR imagery for separating forest-cover types in the Twin Cities metropolitan area (TCMA), MN, USA.

Data and Methods

Study Area

The 770,000-ha study area includes seven counties (Anoka, Carver, Dakota, Hennepin, Ramsey, Scott, and Washington) within the TCMA of Minneapolis-St. Paul, MN, USA. Forest land, most of which is deciduous, constitutes about 90,000 ha (12 percent) of the TCMA (Yuan 2004). We aggregated Yuan's (2004) TCMA map of land cover classes into forest and nonforest classes. The forest/nonforest data set was rescaled to 15-m pixel resolution to accommodate subsequent combinations with 15-m radar data. Subsequent analyses of radar data were constrained to forested pixels of the TCMA.

RADARSAT-1

One 16-bit C-band RADARSAT-1 image, which was acquired June 28, 2001, was used in this study. We performed geometric correction using a 10-m digital elevation model, 60 ground control points, a second-order polynomial, and cubic convolution resampling, which resulted in 15-m pixel spatial resolution, orthorectified (ortho) image. Figure 1 displays backscatter values characteristic of the ortho image: low backscatter (black) portrays open water, high backscatter (white) portrays corner reflectors such as vertical buildings adjacent to horizontal impervious surfaces (white), and intermediate backscatter (gray shades) portrays forest land, cropland, and other land covers.

The resampled image was clipped to the geographic extent of the TCMA study area and was masked to exclude pixels identified as nonforest in the land cover classification. Speckle filtering was performed on the 16-bit ortho image, using a 3-×-3 pixel window Frost speckle filter (Frost *et al.* 1982). A variety of first- and second-order texture measures were computed for 3-×-3 and 5-×-5 windows but only the most promising are discussed here: first-order "variance" (actually, standard deviation) and second-order GLCM dissimilarity. Software limitations prevented the calculation of GLCM second-order texture measures from the 16-bit ortho image, so the image was converted to an unsigned 8-bit image and was histogram-stretched prior to computing first- and second-order texture measures.

Reference Data

Field data used for separability analyses are from the Minnesota Land Cover Classification System (MLCCS) (MDNR 2004). The MLCCS reference data include 19 forest types, in-

Figure 1.—*RADARSAT-1 backscatter image of the Twin Cities metropolitan area, MN, USA, June 28, 2001.*

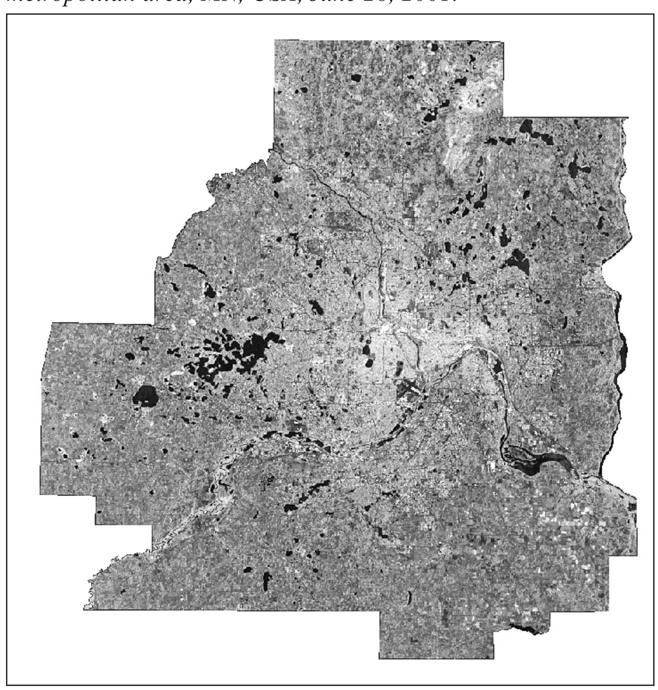

cluding aspen, black ash, box elder, lowland deciduous, maple basswood, red pine, silver maple, tamarack, upland conifer, upland deciduous, and 9 partially overlapping oak subtypes—oak woodland/brushland, oak with impervious cover, white oak, red/white/bur oak, red oak, oak mesic forest, oak forest, oak/mixed deciduous, and bur oak. The oak subtypes were similar to each other so all 9 oak subtypes were aggregated into a single oak class, resulting in 11 MLCCS forest types. Black ash was omitted from first-order texture analyses because covariance matrices for this type were not invertible. Ten forest types were included in first-order analyses and 11 forest types in second-order analyses (table 1).

Forest-Type Class Separability Analyses

We calculated forest-type class separability using average and maximum transformed divergence (TD) values (Jensen 1996). According to Jensen (1996), TD values below 1,700 indicate poor separation, values above 1,900 indicate good separation, and values of 2,000 indicate excellent separation. We assumed that TD values between 1,700 and 1,900 indicate moderate separability.

Results

MLCCS forest types were inseparable when using the 16-bit ortho image, (average TD of 68, maximum TD of 254; table 1). Speckle reduction from the 3×3 Frost filter resulted in average TD of 1,496 and maximum TD of 2,000 (table 1). Average and maximum TD values were 1,716 and 2,000, respectively, before histogram stretching and 1,606 and 2,000, respectively, after histogram stretching of the 8-bit ortho image (table 1). Average and maximum separability of forest types using a first-order texture measure (5-×-5 standard deviation texture after histogram stretching) were 502 and 1,995, respectively (table 1). Forest types were inseparable using a dissimilarity second-order texture measure with a 3-×-3 window and a 3 standard deviation stretch (average TD of 57, maximum TD of 334; table 1).

Discussion

Separability among 1 forest classes increased in TD values after speckle filtering, and was greatest with a 3-×-3 Frost filter. This observation conforms to the results of Kuplich *et al.* (2000), who reported that image filtering produced improved classifications of urban, pasture, and forest classes in Brazil. In addition, rescaling from 16-bit to 8-bit data resulted in markedly improved separability among 11 forest types. First-order texture of 8-bit data appeared to provide separation of forest-type classes, but the separability was no better than using 8-bit data alone. Second-order texture measures appeared to provide little or no separability among pairs of forest types. Although the approach required orthorectification, several image-processing steps, and the availability of a preexisting forest/nonforest land cover classification, RADARSAT-1 imagery can provide for separability among many forest types. This capability may be applied for forest-type mapping, especially where improved discrimination among broad-leaved or needle-leaved types is required or where imagery from optical sensors is degraded by persistent cloud cover.

Table 1.—*Transformed divergence values for RADARSAT-1 imagery and selected derivatives, Twin Cities metropolitan area, MN, USA.*

Type	Band	Texture	Ave.	Max.
16-bit	ortho	none	68	254
16-bit	ortho, 3×3 Frost speckle filter	none	1,496	2,000
8-bit	ortho	none	1,716	2,000
8-bit	ortho, 4 standard deviation stretch	5×5 standard deviation	502	1,995
8-bit	ortho, 3 standard deviation stretch	3×3 dissimilarity	57	334

Ave. = average. Max. = maximum.

Literature Cited

Collins, M.J.; Wiebe, J.; Clausi, D.A. 2000. The effect of speckle filtering on scale-dependent texture estimation of a forested scene. IEEE Transactions on Geoscience and Remote Sensing. 38: 1160-1170.

Frost, V.S.; Stiles, J.A.; Shanmugan, K.S.; Holtzman, J.C. 1982. A model for radar images and its application to adaptive digital filtering of multiplicative noise. IEEE Transactions on Pattern Analysis and Machine Intelligence. 4: 157-166.

Haralick, R.M.; Shanmugam, K.; Dinstein, I. 1973. Textural features for image classification. IEEE Transactions on Systems, Man, and Cybernetics. SMC-3: 610-621.

Huang, H.; Legarsky, J.; Othman, M. 2007. Land-cover classification using RADARSAT and Landsat imagery for St. Louis, Missouri. Photogrammetric Engineering & Remote Sensing. 73: 37-43.

Jensen, J.R. 1996. Introductory digital image processing: a remote sensing perspective. 2nd ed. Upper Saddle River, NJ: Prentice Hall. 316 p.

Kasichke, E.S.; Melack, J.M.; Dobson, M.C. 1997. The use of imaging radars for ecological applications—a review. Remote Sensing of Environment. 59: 141-156.

Kuplich, T.M.; Freitas, C.C.; Soares, J.V. 2000. The study of ERS-1 SAR and Landsat TM synergism for land use classification. International Journal of Remote Sensing. 21: 2101-2111.

Leckie, D.G.; Ranson, K.J. 1998. Forestry applications using imaging radar. In: Henderson, F.M.; Lewis, A.J., eds. Principles and applications of imaging radar (manual of remote sensing). New York: John Wiley: 436-509.

Minnesota Department of Natural Resources (MDNR). 2004. Minnesota Land Cover Classification System user manual. Version 5.4. Minnesota Department of Natural Resources, Central Region. 273 p. http://files.dnr.state.mn.us/assistance/nrplanning/community/mlccs/mlccs_manual_v5_4.pdf. (9 November 2006).

Päivinen, R.; Lehikoinen, M.; Schuck, A.; Häme, T.; Väätäinen, S.; Kennedy, P.; Folving, S. 2001. Combining Earth observation data and forest statistics. Res. Rep. 14. Joensuu, Finland: European Forest Institute, Joint Research Center—European Commission. 101 p.

Powell, D.S.; Faulkner, J.L.; Darr, D.R.; Zhu, Z.; MacCleery, D.W. 1993. Forest resources of the United States, 1992. Gen. Tech. Rep. RM-234. Fort Collins, CO: U.S. Department of Agriculture, Forest Service, Rocky Mountain Forest and Range Experiment Station. 132 p.

Ranson, K.J.; Williams, D.L. 1992. Remotely sensed technology for forest ecosystem analysis. In: Shugart, H.H.; Leemans, R.; Bonan, G.B., eds. A systems analysis of the global boreal forest. New York: Cambridge University Press: 267-290.

Yuan, F. 2004. Remote sensing and GIS-based regional land-cover mapping and change analysis in the Twin Cities metropolitan area. St. Paul, MN: University of Minnesota. 131 p. Ph.D. dissertation.

Zhu, Z.; Evans, D.L. 1994. U.S. forest types and predicted percent forest cover from AVHRR data. Photogrammetric Engineering & Remote Sensing. 60: 525-531.